LETTERS

ASC is a Bax adaptor and regulates the p53–Bax mitochondrial apoptosis pathway

Takao Ohtsuka[1], Hoon Ryu[2], Yohji A. Minamishima[1], Salvador Macip[3], Junji Sagara[4], Keiichi I. Nakayama[5], Stuart A. Aaronson[3] and Sam W. Lee[1,6]

The apoptosis-associated speck-like protein (ASC) is an unusual adaptor protein that contains the Pyrin/PAAD death domain in addition to the CARD protein–protein interaction domain[1–5]. Here, we present evidence that ASC can function as an adaptor molecule for Bax and regulate a p53–Bax mitochondrial pathway of apoptosis. When ectopically expressed, ASC interacted directly with Bax, colocalized with Bax to the mitochondria, induced cytochrome *c* release with a significant reduction of mitochondrial membrane potential and resulted in the activation of caspase-9, -2 and -3. The rapid induction of apoptosis by ASC was not observed in Bax-deficient cells. We also show that induction of ASC after exposure to genotoxic stress is dependent on p53. Blocking of endogenous ASC expression by small-interfering RNA (siRNA) reduced the apoptotic response and inhibited translocation of Bax to mitochondria in response to p53 or genotoxic insult, suggesting that ASC is required to translocate Bax to the mitochondria. Our findings demonstrate that ASC has an essential role in the intrinsic mitochondrial pathway of apoptosis through a p53–Bax network.

The apoptosis-associated speck-like protein, designated ASC, has recently emerged as an important regulator of apoptosis, immune response and breast cancer development[2–5]. ASC belongs to a large family of proteins that contain a Pyrin, AIM and death-domain-like (PAAD) domain[1,2,5]. *ASC* consists of an amino-terminal Pyrin followed by the carboxy-terminal caspase recruitment domain (CARD), representing one of only two genes in the human genome that encodes a protein combining these two protein interaction domains[1,2,4]. *ASC* is also known as TMS (target of methylation-induced silencing) and is inactivated in ~40% of breast cancers[3]. Recently, it has been reported that ASC can inhibit diverse NF-κB induction pathways by exerting effects on the IKK complex in response to various pro-inflammatory stimuli, including tumour necrosis factor α (TNFα), interleukin-1β (IL1β) and lipopolysaccharide (LPS)[4]. ASC-mediated apoptosis proceeds through a CARD-dependent aggregation step followed by activation of a caspase-9 (ref. 6), whereas ASC regulates Fas-mediated death signalling in immune cells[7]. These studies suggest that ASC is most probably involved in both mitochondria- and death-receptor-mediated apoptotic pathways.

We identified *ASC* as a tumour suppressor p53-responsive gene through a DNA chip expression array that compared gene expression in the presence or absence of p53. ASC mRNA and protein expression was induced in response to p53 or DNA damage in cells containing wild-type p53 with kinetics similar to those of the p53-dependent gene, *p21^{Waf1}* (Fig.1a). Of note, inhibition of p53 activation in response to DNA-damaging agents by siRNA targeting p53 abrogated ASC induction (Fig. 1a). We detected a potential p53 recognition sequence that exhibited an 85% match to the consensus p53-binding sequence at nucleotides −299 to −320 in the *ASC* promoter region. To determine if p53 could bind to this potential p53-binding site *in vivo*, we used a chromatin immunoprecipitation (ChIP) assay to analyse cell lysates extracted from Saos2 cells infected with adenovirus expressing wild-type p53. The 225-bp *ASC* genomic fragment containing a candidate p53-binding site was specifically precipitated as a p53 protein–DNA complex with an anti-p53 antibody, but not with anti-haemagglutinin (HA) antibody (Fig. 1b). Amplification of a region containing a p53-binding site in the *p21^{Waf1}* promoter served as a positive control. In addition, an electrophoretic mobility shift assay with an oligonucleotide containing this putative p53-binding site confirmed the specificity of p53 binding (Fig. 1c). In addition, two copies of the potential ASC p53-binding site in a pGL3 promoter vector showed a significant increase in luciferase activity in response to p53 (Fig. 1d).

A number of p53 target-genes that can mediate p53-dependent cell cycle arrest or cell death have been identified[8,9]. Thus, we initially examined whether ectopic expression of ASC affected cell growth or survival in the human colon carcinoma cell line, HCT116. Ectopic expression of ASC in HCT116 cells caused significant apoptosis (Fig. 2a). ASC expression resulted in a marked increase in the sub-G1 population from ~2%

[1]Cancer Biology Program, Hematology/Oncology Division, Beth Israel Deaconess Medical Center and Harvard Medical School, Boston, MA 02115, USA. [2]Department of Neurology, Boston University School of Medicine, The Geriatric Research Education and Clinical Center, Bedford, MA 01730, USA. [3]Derald H. Ruttenberg Cancer Center, Mount Sinai School of Medicine, New York, NY 10029, USA. [4]Department of Molecular Oncology and Angiology, Shinshu University School of Medicine, Matsumoto, Nagano 390-8621, Japan. [5]Departments of Molecular and Cellular Biology, Medical Institute of Bioregulation, Kyushu University, 3-1-1 Maidashi, Higashi-ku, Fukuoka, Fukuoka 812-8582, Japan.
[6]Correspondence should be addressed to S.W.L. (e-mail: slee2@caregroup.harvard.edu).
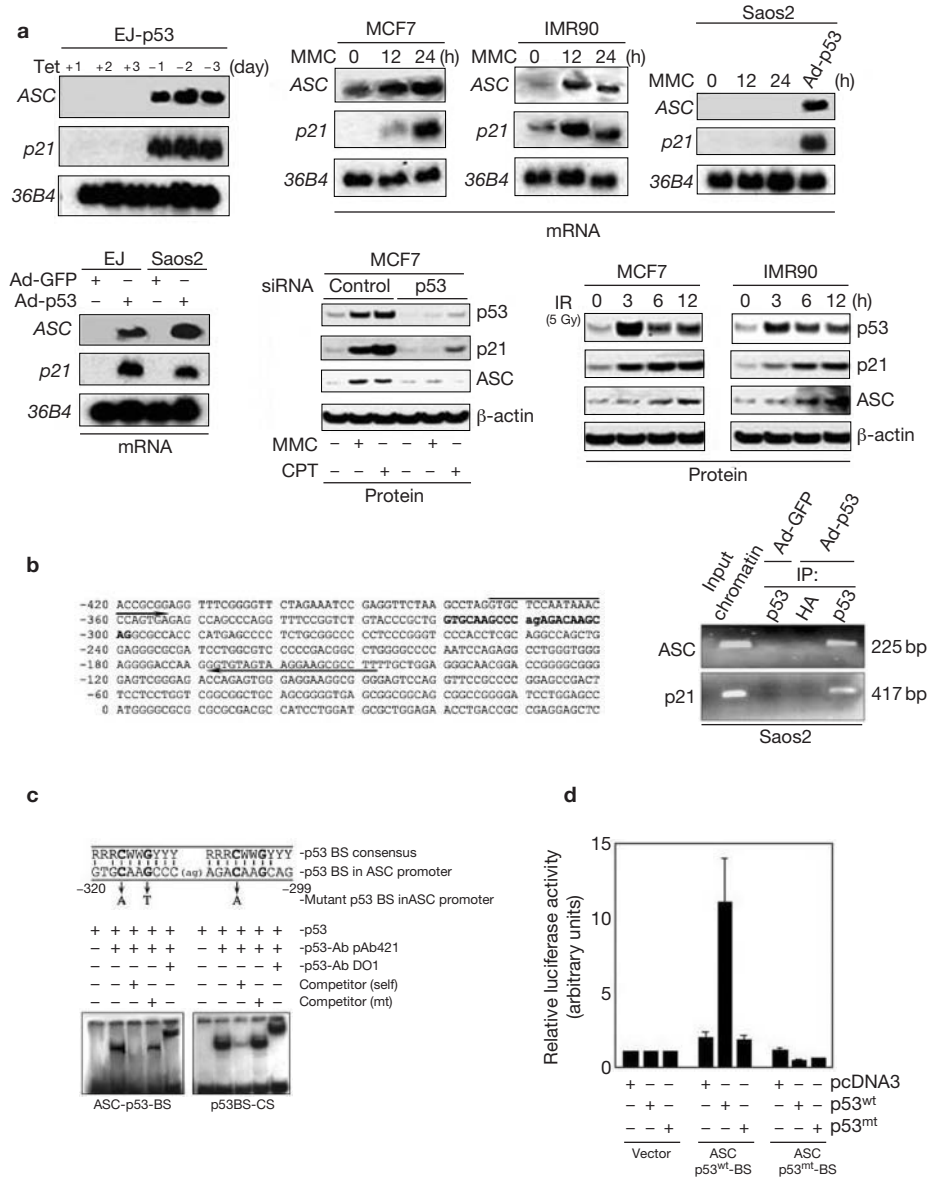
Figure 1 p53-dependent induction of ASC. (**a**) ASC expression is inducible with p53. Left panels show induction of *ASC* mRNA after removal of tetracycline (tet) in EJ-p53 cells and after infection with recombinant adenovirus, Ad-p53, in EJ or Saos-2 cells. Northern blots were performed sequentially using ^{32}P-labelled probe against ASC, p21 and 36B4 (loading control). Right panels show that induction of ASC in response to DNA damage is p53-dependent. MCF7 cells were transfected with siRNA oligos targeting wild-type p53 or control siRNA oligos (luciferase) for 2 days, then exposed to DNA-damaging agents, MMC and CPT, respectively, for 24 h. Western blots were performed using antibodies against p53, p21, ASC and β-actin. MCF7 and IMR90 cells were also irradiated with 5 Gy in a γ-irradiator with a mark [135]I Cs source. (**b**) ChIP assay of p53 DNA-binding activity in p53-expressing Saos2 cells and parental p53-null Saos2 cells. p53-null Saos2 cells were infected with adenovirus expressing p53 or GFP for 24 h. Next, ChIP assay was performed using anti-p53 or -HA antibody (negative control). Amplification products were 225 bp (ASC) and 417 bp (p21/Waf1: positive control), respectively. A sequence map of the ASC promoter region containing the primers (shown as arrows) and a p53-responsive element (bold) is also shown. (**c**) Electrophoretic mobility shift assays (EMSA) of a potential p53-binding site (BS). In the designated lanes, p53 antibodies pAb421 and/or pAbDO1 were included. Interaction between p53 and DNA was inhibited by a hundredfold excess of unlabelled oligonucleotides corresponding to the binding site of the ASC p53-BS, but not by mutated p53-BS oligonucleotides. EMSA assay using the consensus p53-BS probe was also performed, and the interaction was inhibited by unlabeled p53-BS. A putative p53 recognition site located in the promoter region of the *ASC* gene (from −299 to −320) is shown. Required bases for the p53-BS are shown in bold (c and g). (**d**) Luciferase assay. Two constructs containing two copies of the possible 22-bp p53-BS with 5-bp interval or two mutated copies of the 22-bp p53-BS were cloned into a luciferase reporter vector (pGL3-promoter vector) containing the SV40 minimal promoter. ASC-p53-BS mutant reporter vector contains three point mutations. Saos2 cells were cotransfected with either of these constructs, pRL-CMV vector and either wild-type p53 or mutant p53 expression construct (pcDNA3-p53[wt] or -p53[mt]), as well as control reporter vector.

to ~38%. In addition, cell death, as measured by trypan blue exclusion, increased from ~4% in Ad-green fluorescent protein (GFP)-infected control cells to >50% in Ad-ASC-infected cells 48 h after infection. As

p53 is also known to induce Bax, a pro-apoptotic protein that causes mitochondrial dysfunction[10–12], we also examined the effects of ASC in an isogenic derivative of HCT116, in which Bax had been deleted by
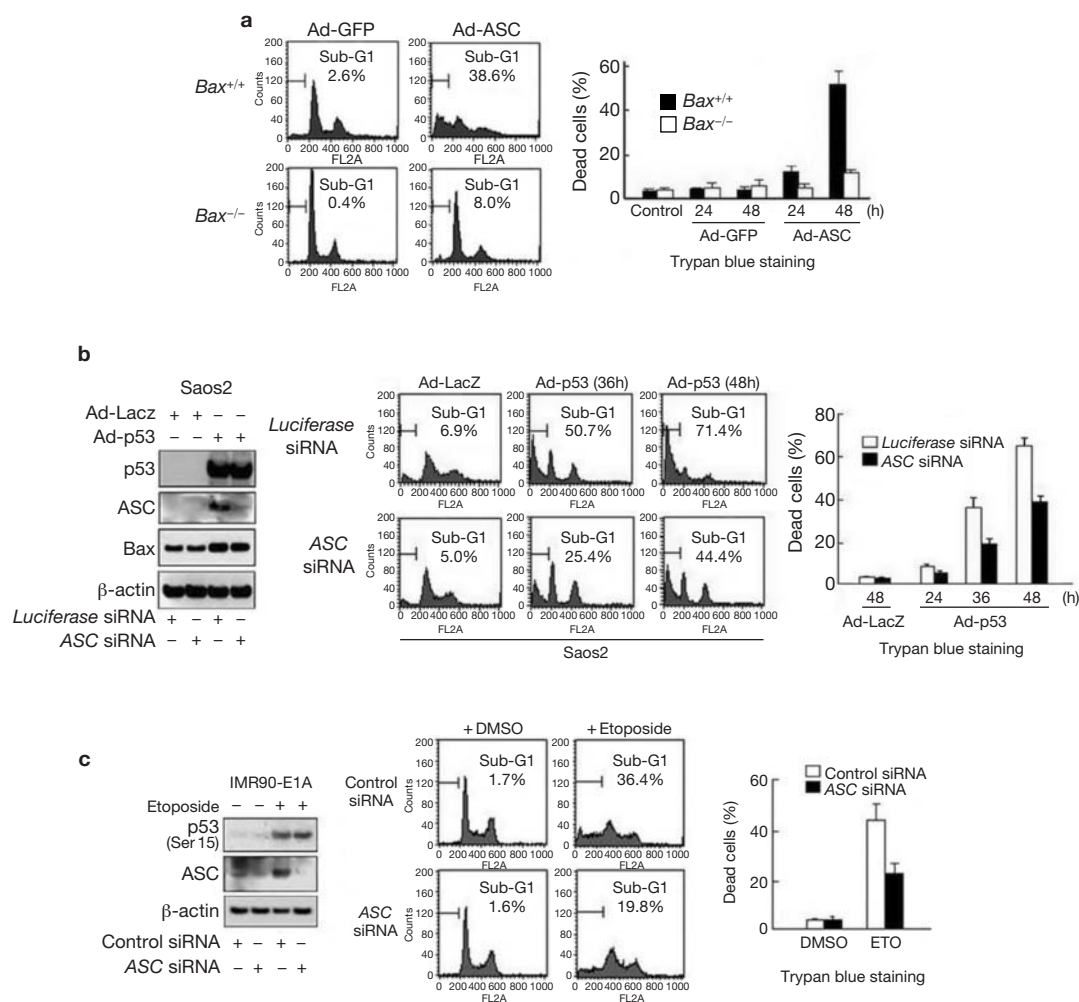
Figure 2 Bax is essential for cell death mediated by ASC. (**a**) ASC-mediated apoptosis in *Bax⁺/⁺* or *Bax⁻/⁻* HCT116 cells. HCT116 cells were infected with Ad-ASC or Ad-GFP at an MOI of 20. The apoptotic population (indicated by sub-G1) was then measured by FACS analysis. The percentage of dead cells was also measured by Trypan blue staining of *Bax⁺/⁺* and *Bax⁻/⁻* HCT116 cells infected with Ad-ASC or Ad-GFP at a MOI of 20 for 24 and 48 h. (**b**) Effect of ASC inhibition on p53-mediated apoptosis. Saos-2 cells were transfected with *ASC* siRNA or *luciferase* siRNA (control) then infected with adenovirus expressing LacZ or p53 at a MOI of 20. Left panel: a western blot showing inhibition of ASC induction in response to p53 by *ASC* siRNA. After adenovirus infection, cells were harvested for flow cytometry analysis at the indicated times (36 and 48 h). The apoptotic population

(sub-G1 population) was then measured. The percentage of dead cells was also measured by Trypan blue exclusion analysis at the indicated times. (**c**) ASC repression compromizes p53—dependent apoptotic response to chemotherapeutic drugs. IMR90-E1A cells were transfected with siRNA oligonucleotides targeting ASC or control siRNA oligos (luciferase) for 2 days, then treated with etoposide (50 μM) for 12 h. Western blots were then performed to determine levels of p53 (phospho-p53, Ser 15), ASC and β-actin. The apoptotic population (sub-G1 population, middle panel) was measured by FACS analysis using the same cells. The percentage of dead cells was also measured by Trypan blue exclusion analysis (right panel). In all cases, error bars indicate ± SD of three independent experiments with duplicate plates.

homologous recombination[13]. The apoptotic effect of ASC was significantly reduced in Bax-null cells (Fig. 2a). ASC-induced apoptosis was also observed in other human cancer cell lines independent of their p53 status (data not shown). We also examined the effects of ASC overexpression on apoptotic responses to the genotoxic agents, etoposide and indomethacin. ASC overexpression resulted in a marked increase in apoptosis in the presence of either agent in wild-type cells, and to a lesser extent in Bax-null cells (see Supplementary Information, Fig. S1a). These findings imply that ASC not only functions in Bax-mediated apoptosis, but must also function in Bax-independent apoptotic pathways.

To investigate whether ASC induction in response to p53 or genotoxic stress contributes directly to p53- or stress-mediated apoptosis, we used *ASC* siRNA to suppress the expression of endogenous ASC

induced by p53 or genotoxic stress. Transfection of *ASC* siRNA resulted in the suppression of ASC expression in Ad-p53-infected Saos2 cells, compared with cells transfected with control siRNA (luciferase-specific; Fig. 2b, left). Moreover, this reduction of ASC expression resulted in a reproducible decrease in p53-mediated apoptosis, compared with that observed in cells in which a control siRNA was introduced (Fig. 2b, middle and right panels). Recent studies have shown that the E1A adenoviral oncogene can sensitize IMR90 normal fibroblasts to genotoxic drugs by promoting the activation of Bax and caspase-9 (ref. 14). To test whether apoptosis requires ASC, siRNA was used to suppress expression of endogenous ASC induced by apoptosis drugs in IMR90-E1A fibroblasts. A siRNA against ASC efficiently inhibited ASC expression in IMR90-E1A cells, whereas control siRNA
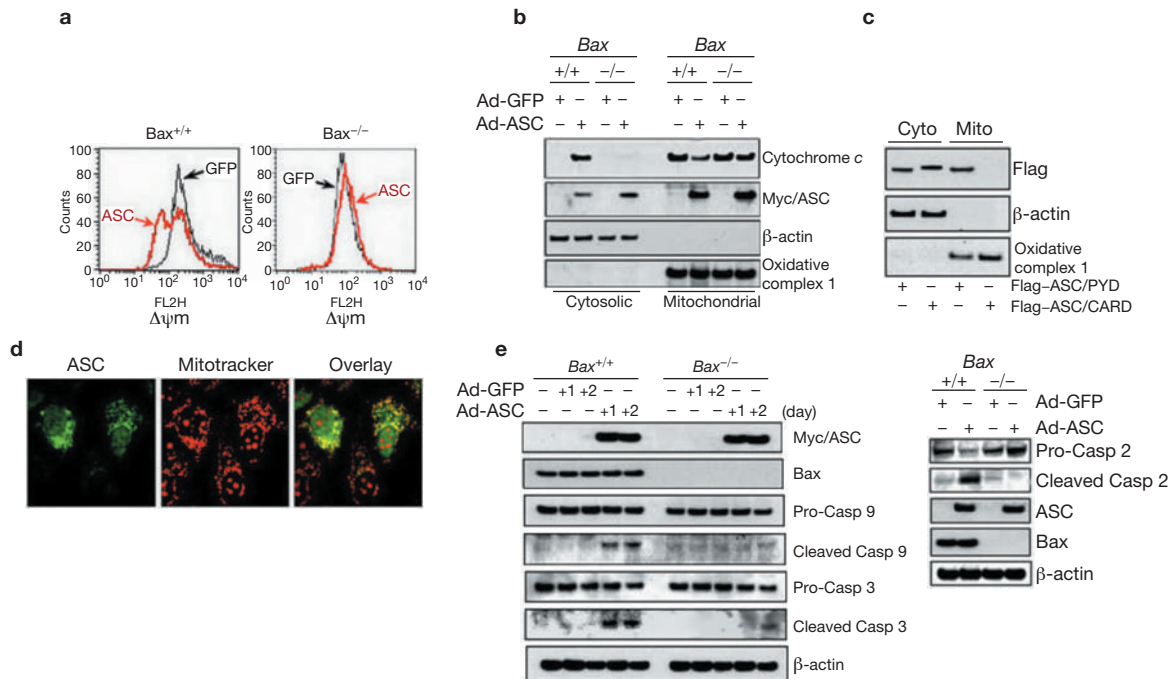
Figure 3 ASC requires Bax to regulate mitochondrial apoptosis. (**a**) ASC induces dissipation of the mitochondrial membrane potential in $Bax^{+/+}$ cells. $Bax^{+/+}$ and $Bax^{-/-}$ HCT116 cells were infected with Ad-ASC (red line) or Ad-GFP (black line); 36 h after infection, cells were stained with MitoTraker (red) to measure membrane potential. Cells were then analysed by flow cytometry. Data was analysed by gating the infected cell population and plotting red fluorescence. (**b**) ASC induces cytochrome c release in $Bax^{+/+}$ cells. $Bax^{+/+}$ and $Bax^{-/-}$ HCT116 cells were infected with Ad-ASC or Ad-GFP. Protein extracts were divided into cytosol and mitochondrial fractions and analysed by western blotting with antibodies against cytochrome c and Myc. Fractionation quality was verified by controlling the distribution of specific subcellular markers (β-actin as a cytoplasm-specific marker, and oxidative complex I protein as mitochondria-specific marker). (**c**) The pyrin domain of ASC is essential for translocation of ASC to mitochondria. U2OS cells were transfected with plasmids encoding Flag–ASC/CARD (Pyrin-domain-deleted) or Flag-tagged ASC/PYD (CARD

deleted). Protein extracts were divided into cytosol and mitochondrial fractions and analysed by anti-Flag western blotting. Fractionation quality was verified by controlling the distribution of specific subcellular markers, as mentioned above. (**d**) ASC localization at mitochondria. Myc–ASC (green) was expressed in MCF7 cells and visualized by confocal microscopy. MitoTracker (red dye) was used to visualize the mitochondria. An overlay is also shown. (**e**) Caspase-9, -2 and -3 activation by ASC. Caspase-9 and -3 activations were determined with cell extracts from $Bax^{+/+}$ or $Bax^{-/-}$ HCT116 cells at the indicated times after infection with Ad-ASC or Ad-GFP by western blotting with antibodies against caspase-9 and -3. The unprocessed caspase-9 or -3 and the cleaved 37K or 17K product of the active caspase-9 or -3 are indicated. Right panel: ASC activates caspase-2 in a Bax-dependent manner. $Bax^{+/+}$ or $Bax^{-/-}$ HCT116 cells were infected with Ad-ASC or Ad-GFP. 48 h after infection, cell lysates were prepared for western blotting with antibodies against procaspase-2, cleaved caspase-2, Myc–ASC, Bax and β-actin.

against luciferase had no effect on the expression of ASC (Fig. 2c, left panel). In IMR90-E1A cells, inhibition of ASC expression by siRNA significantly inhibited apoptosis induced by etoposide (Fig. 2c, middle and right panels). siRNA was also used to suppress ASC expression in DNA-damage-treated MCF7 cells. The siRNA to ASC inhibited apoptosis induced by the DNA-damaging agent camptothecin (see Supplementary Information, Fig. S2). In addition to Bax, another pro-apoptotic Bcl2-family protein, Bak, can initiate mitochondrial dysfunction and apoptotic death[11,15–17], and the presence of either Bax or Bak seems to be essential for the mitochondrial pathway of apoptosis. To assess the role of Bak in ASC-induced apoptosis, we determined whether inhibition of Bak expression had an effect on ASC-mediated apoptosis in $Bax^{+/+}$ or $Bax^{-/-}$ HCT116 cells. Whereas the Bak siRNA efficiently silenced Bak expression, knock-down of Bak expression did not affect ASC-induced apoptosis (see Supplementary Information, Fig. S1b), indicating that Bak is not required for ASC-mediated apoptosis. These findings imply that ASC functions as a downstream effector of p53 in DNA-damage-mediated apoptosis.

Bax induces the release of apoptotic stimulators, such as cytochrome c and Smac/Diablo, and causes mitochondrial dysfunction[12,16,18,19].

Disruption of the mitochondrial membrane potential, $\Delta\Psi$m, with the consequent release of cytochrome c to the cytoplasm, constitutes a critical step in the mitochondrial apoptotic pathway[11,12,19]. As ASC-induced apoptosis was mainly Bax-dependent, we examined the mitochondrial $\Delta\Psi$m, an integral component of mitochondrial membrane function, after expression of ASC or GFP (control) by Ad-ASC or Ad-GFP. A significant reduction of membrane potential was detected in $Bax^{+/+}$ cells expressing ASC, but not in Bax-null cells under the same conditions (Fig. 3a). We also determined the effects of ASC on the release of cytochrome c in $Bax^{+/+}$ and $Bax^{-/-}$ cells. Cytosolic and mitochondrial extracts were separated by biochemical fractionation through homogenization. ASC induced translocation of cytochrome c to the cytoplasm in $Bax^{+/+}$ cells, but negligible cytochrome c release was detected in $Bax^{-/-}$ cells (Fig. 3b). Of note, immunoblot analysis of subcellular fractions showed that most of the ectopically expressed ASC protein (Myc–ASC) was located in the mitochondrial fraction. Fractionation quality was verified by controlling the distribution of specific subcellular markers (β-actin as a cytoplasm-specific marker, and oxidative complex I protein as a mitochondria-specific marker).

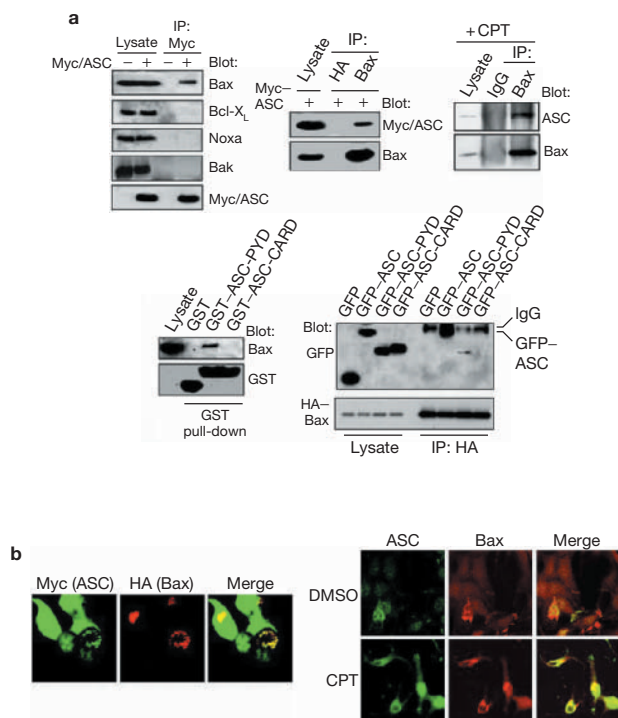To determine which specific region of ASC was responsible for its

Figure 4 ASC protein is associated with Bax, but not with other members of the Bcl2 family. (**a**) U2OS cells were transfected with Myc–ASC. After 36 h, cell extracts were immunoprecipitated (IP) with the anti-Myc antibody and analysed by western blotting (WB) with antibodies against Bax, Bcl-X$_L$, Noxa or Bak. Reverse immunoprecipitation experiments with anti-Bax were also performed with the same cell lysates and analysed by anti-Myc western blotting. As a negative control, the same cell lysate was also immunoprecipitated with the anti-HA antibody before western blotting with anti-Myc and -Bax antibodies. Co-immunoprecipitation of endogenous Bax with ASC from Myc–ASC-transfected U2OS cell extracts was clearly observed, but no interaction was found between ASC and Bcl-X$_L$, Bak or Noxa proteins. Interaction between endogenous Bax and endogenous ASC proteins was then examined by immunoprecipitation experiments. MCF7 cells were exposed to CPT for 24 h to induce ASC expression, and cell lysates were prepared for immunoprecipitation using anti-Bax (6A7) and mouse IgG, respectively, before western blotting with antibodies against ASC and Bax. Interaction between ASC and Bax was also confirmed by *in vitro* binding assay using GST–ASC-PYD domain (deleted amino acid 101–195) or GST–ASC-CARD (deleted amino acid 1–100). The GST pull-down assay with purified GST–ASC fusion proteins and 500 μg of cell lysates was performed and followed by immunoblotting with the anti-Bax antibody. The Bax-binding region in the ASC protein was identified (right panel). HA–Bax and GFP–ASC, GFP–ASC-PYD or GFP–ASC-CARD were co-expressed in U2OS cells. Cell lysates were analysed by immunoprecipitation with anti-HA before anti-GFP western blotting. Of note, GFP–ASC/Pyrin was immunoprecipitated with HA–Bax. (**b**) Co-distribution of ASC and Bax in MCF7 cells. MCF7 cells were cotransfected with Myc–ASC and HA–Bax. Transfected cells were immunostained with anti-Myc (green) and counterstained with anti-HA (red) before visualization by confocal microscopy. To visualize the colocalization of endogenous ASC with endogenous Bax, MCF7 cells were treated with CPT, stained with anti-ASC monoclonal (green) and anti-Bax polyclonal (red) antibodies before visualization by confocal microscopy.

translocation to mitochondria, truncated deletion mutants of ASC were generated, each containing a Pyrin or CARD region: Flag–ASC/PYD (deleted CARD domain, amino acids 101–195) and Flag–ASC/CARD (deleted N-terminal Pyrin domain amino acids

1–100). Expression constructs of these Flag-tagged deletion mutants were transfected into U2OS cells and subcellular fractionation analysis was performed. The mitochondrial fraction from these cell extracts contained the Pyrin-containing fragments, but the Pyrin-deleted ASC mutant containing the CARD region was not detected in the mitochondrial fraction (Fig. 3c). These results demonstrate that the N terminus Pyrin region is required for translocation of ASC to the mitochondria. To further characterize the subcellular localization of ASC, we transfected a Myc-tagged ASC expression construct, pcDNA3-ASC-Myc, into MCF7 cells and performed immunostaining for the Myc-tagged protein. Confocal microscopy showed that ASC strongly stained in a dotted pattern in the cytoplasm and colocalized with the mitochondrial marker, MitoTracker (Fig. 3d). We next examined whether ASC affected any caspases. Ectopic expression of ASC resulted in the cleavage of procaspases-9, -3 and -2 to the active forms in $Bax^{+/+}$ cells (Fig. 3e), whereas ASC failed to produce detectable levels of cleaved caspase-9 or -2 and only induced slightly induced caspase-3 cleavage in Bax-deficient cells. These results strongly imply that ASC localizes to the mitochondria and induces apoptosis mainly through a Bax-dependent mitochondrial pathway.

It is known that translocation of Bax to the mitochondrial outer membrane is required to release cytochrome *c* during apoptosis induced by various death stimuli, but the mechanism of Bax translocation to the mitochondria is unclear. Bax and ASC are both regulated by p53 and share other properties, such as cytoplasmic and mitochondrial localization, pro-apoptotic function and functional cooperation in apoptosis. Thus, we explored the possibility that ASC interacts with Bax, and that this interaction may be required in the p53–Bax-intrinsic mitochondrial pathway of apoptosis. ASC co-immunoprecipitated with Bax but failed to form a complex with Bcl-X$_L$, Noxa, Bak (Fig. 4a, top) or Bcl2 (data not shown). Endogenous ASC also interacted with endogenous Bax in DNA-damage-treated MCF7 cells (Fig. 4a, upper right panel). To confirm the binding of Bax to ASC and to identify the domain responsible, two GST fusion proteins were generated, each containing a Pyrin or CARD region. A GST pull-down assay was performed by using the two purified GST–ASC fusion proteins and 500 μg of cell lysate followed by immunoblotting with Bax antibody. The results show that the ASC Pyrin domain (amino acids 1–100) bound to Bax (Fig. 4a, lower left panel), whereas binding of the C-terminal CARD region of ASC to Bax was not detectable. To confirm the specific interaction of Bax with the ASC Pyrin domain *in vivo*, GFP was fused to each region of ASC using a pEGFP plasmid to generate pEGFP-Pyrin (GFP–ASC-PYD) and pEGFP-CARD (GFP–ASC-CARD). GFP–ASC-full-length, GFP–ASC-PYD or GFP–ASC-CARD were transiently cotransfected with HA–Bax into U2OS cells. Protein interactions were assessed by immunoprecipation with a HA-tagged antibody before western blot analysis with a GFP-specific antibody. Bax binds to the Pyrin region of ASC, but not to the CARD region of ASC (Fig. 4a, lower right panel). We also investigated whether Bax colocalizes with ASC. Ectopic co-expression of ASC and Bax in MCF7 cells demonstrated their colocalization in the cytoplasm (Fig. 4b, left panel). Colocalization of endogenous ASC with endogenous Bax was also confirmed by immunohistochemical experiments in MCF cells treated with a DNA damaging agent, CPT (Fig. 4b, right panel). The two proteins were more clearly co-distributed in DNA-damage-treated cells. These results indicate that ASC interacts with Bax in the cytoplasm, and the punctate pattern observed was consistent with their colocalization at mitochondria.

To examine the involvement of ASC in the translocation of Bax to the mitochondria, pcDNA3-ASC/Flag or vector alone was transiently transfected into U2OS cells. After 36 h, cytosolic and mitochondrial extracts were separated by biochemical fractionation.
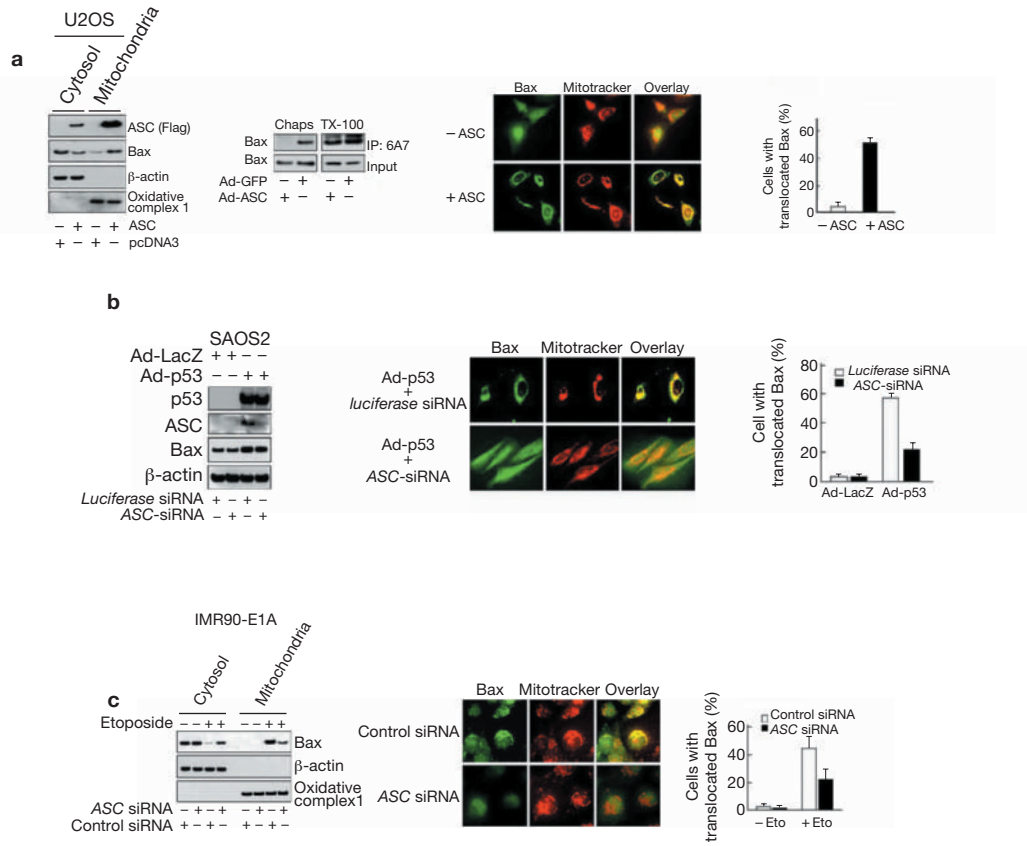
Figure 5 Effect of ASC on p53- or DNA damage-induced Bax translocation. (**a**) ASC-mediated translocation of Bax to mitochondria. U2OS cells were transfected with ASC–Flag or vector alone (pcDNA3) and separated into cytosol and mitochondria-rich fractions. All fractions were adjusted to the same volume and analysed by western blotting with antibodies to Myc (ASC), Bax, β-actin (cytosol marker) and oxidative complex-I (mitochondrial marker; left panel). The second panel shows that ASC promotes the conformational change of the Bax protein. U2OS cells were infected with Ad-GFP or Ad-ASC, then cells were lysed in the presence of Chaps or Triton X-100 and immunoprecipitated with anti-Bax monoclonal antibody (clone 6A7) before anti-Bax (N-20) western blotting. Right panels: translocation of Bax to the mitochondria by ASC. ASC or vector alone (pcDNA3) was transfected into U2OS cells and immunostained with Bax antibody (green). Mitochondria were stained with MitoTracker (red); the two images were overlaid (orange-yellow). Bax translocation was determined by counting 100–150 cells for each cell population and is presented in the right panel. (**b**) ASC inhibition abrogates p53-mediated Bax translocation to the mitochondria. Saos-2 cells were transfected with siRNA. After 36 h, cells were infected with Ad-p53 and incubated for an additional 24 h. Left panel:

western blot analysis after inhibition of ASC induction in response to p53 by *ASC* siRNA. Middle panel: cells were co-stained with Bax antibodies (green) and MitoTracker (red) for mitochondria; the two images were overlaid (orange–yellow). Right panel: Bax translocation was determined by counting 100–150 cells for each cell population. Error bars in **a** and **b** indicate ± SD of three independent experiments. (**c**) ASC regulates the translocation of Bax from the cytoplasm to the mitochondria. IMR90-E1A cells were transfected with siRNA to either ASC or luciferase. After 2 days, cells were treated with etoposide (50 μM) or left untreated. Left panel: 12 h after treatment, cells were separated by biochemical fractionation into cytosolic and mitochondrial extracts and analysed for Bax levels by western blotting with antibodies against Bax and specific subcellular markers (β-actin as a cytoplasm marker; oxidative complex I protein as a mitochondria marker, upper left panel). Right panel: inhibition of ASC by siRNA prevents drug-induced Bax translocation to mitochondria. IMR90-E1A cells transfected with *ASC* or *luciferase* siRNA were treated with etoposide for 8 h before fixation for immunostaining with antibodies to Bax (green). Mitochondria were stained with MitoTracker (red). The two images were overlaid (orange-yellow).

Ectopically expressed ASC increased the translocation of Bax to mitochondria, and immunoblot analysis detected lower amounts of endogenous Bax in the cytoplasm (Fig. 5a, upper left panel). In contrast, cells transfected with control vector showed that most of the endogenous Bax protein was located in the cytosolic fraction. It is well-established that the apoptotic signal can induce a conformational change of the Bax protein, resulting in exposure of the Bax N terminus before mitochondrial translocation, and that this conformational change can be detected with an anti-Bax monoclonal antibody clone 6A7 (refs 20–22). Therefore, we tested whether ASC could trigger the same type of conformational change in Bax, as detected in apoptosis-induced cells. We observed

increased binding of the 6A7 antibody to Bax after expression of exogenous ASC, but not GFP (Fig. 5a, middle panel), suggesting that ASC causes a conformational change in Bax. Co-immunostaining of endogenous Bax protein and Mitotracker was also performed to examine the effect of ASC on Bax subcellular localization and translocation to the mitochondria. Bax protein in ASC-transfected cells showed mitochondrial distribution, whereas Bax in control-transfected cells showed a diffuse cytosolic distribution pattern (Fig. 5a, right panel). Quantification of cells displaying mitochondrial Bax staining patterns demonstrated that Bax was translocated to the mitochondria in >50% of ASC-transfected U2OS cells (Fig. 5a, right panel).

To investigate whether ASC induction in response to p53 or geno-toxic stress contributes directly to Bax activation/translocation, *ASC* siRNA was used to suppress the expression of endogenous ASC induced by p53 or genotoxic stress. Transfection of *ASC* siRNA resulted in the suppression of ASC expression in Ad-p53-infected Saos2 cells, compared with cells transfected with control siRNA (luciferase-specific; Fig. 5a, left panel). Inhibition of ASC expression was associated with a >50% reduction of Bax translocation to mito-chondria (Fig. 5b, middle and right panel). To further examine whether ASC induction in response to genotoxic stress contributes directly to Bax activation/translocation, we also used siRNA to sup-press the expression of endogenous ASC. Transfection of *ASC* siRNA resulted in the suppression of genotoxic stress-induced translocation of Bax to the mitochondria in etoposide-treated IMR90-E1A cells, compared with cells transfected with control siRNA (luciferase-spe-cific; Fig. 5c, right panel). Biochemical fractionation experiments also showed that inhibition of ASC suppressed translocation of Bax to the mitochondria by ~50% (Fig. 5c, left panel). Moreover, inhibition of ASC inhibited the conformational change in Bax induced by etoposide (see Supplementary Information, Fig. S3). We also used siRNA to sup-press ASC expression in DNA-damage-treated MCF7 cells. The siRNA to ASC inhibited Bax translocation and apoptosis induced by a DNA-damaging agent, camptothecin (see Supplementary Information, Fig. S2). All of these findings imply that ASC functions as a down-stream effector of p53 in DNA-damage-mediated apoptosis, and that ASC regulates the intrinsic apoptosis pathway through a p53–Bax mitochondrial pathway.

We have shown here that ASC is induced in response to p53 and DNA damage. ASC interacts functionally and physically with Bax to promote Bax translocation to the mitochondria, and apoptosis associated with the release of cytochrome *c* and the activation of caspase-9, -2 and -3. Our findings suggest a new network in which ASC is important for reg-ulating the Bax-intrinsic mitochondrial pathway in both a p53-depend-ent and -independent manner. Recent evidence has implicated an alternative pathway in the control of apoptosis, in which caspase-1 and -7 can be activated in response to an apoptotic stimulus in the absence of amplification of the apoptosome[23]. As it was reported that ASC binds and activates caspase-1, ASC may also induce apoptosis through this alternative pathway. It has also been reported that ASC was induced by TNFα, as well as by anti-Fas antibody or Fas ligand, and that the sus-tained increase of ASC by Fas-mediated death signalling requires activa-tion of caspases and further enhances the apoptotic processes in immune cells[7]. Other studies indicate that the pyrin domain of ASC interacts physically with caspase-8 and pyrin in a competitive manner, and that ASC-mediated apoptosis is inhibited by a mutant form of cas-pase-8 (ref. 24). This is consistent with our observations that inhibition of ASC expression reduced TNFα-induced apoptosis (see Supplementary Information, Fig. S4). Therefore, although ASC is a crit-ical mediator of Bax-dependent apoptosis, it is probable that ASC regu-lates caspase activation programmes independently of Bax as well. Further studies are needed to elucidate the mechanisms by which ASC may influence the extrinsic death process. Recent studies have shown that caspase-2 activation is required for the translocation of Bax to the mitochondria, as well as for release of the mitochondrial proteins cytochrome *c* and Smac/Diablo, and activation of caspase 9, which func-tions downstream of the mitochondrial apoptosis pathway[25]. Although ectopically expressed ASC induced cleavage of caspase-2 in $Bax^{+/+}$ cells, but not in $Bax^{-/-}$ HCT116 cells, it remains to be elucidated if ASC can be implicated in caspase-2-mediated Bax activation and apoptosis.

Recent studies suggest that there is a cytoprotective mechanism that negatively regulates the mitochondrial translocation of Bax through Bax–Ku70 (ref. 26) and/or Bax–Humanin[27]. Binding of ASC to Bax may protect Bax from Ku70- or Humanin-peptide-mediated inactiva-tion of Bax. ASC/TMS1 is a major target of methylation-induced gene silencing in human breast cancer[3,28]. Thus, it is possible that the sup-pression of ASC expression and failure of the concurrent downstream signalling confer a survival advantage by allowing tumour cells to escape apoptosis. A more detailed understanding of the molecular interactions involving ASC and its partners may offer the opportunity to mimic its functions and, thus, potentiate the apoptotic effects of current agents used in cancer therapy. □

METHODS

Plasmids, adenovirus and GST constructs. Mammalian expression vector con-structs encoding Flag–ASC, GFP–ASC, Myc–ASC and deletion mutants (Δ1–100, ASC-CARD; and Δ101–195, ASC-PYD) of ASC have been described[3,29]. Adenovirus expressing Myc-tagged ASC (Ad-ASC) was gener-ated, amplified and titrated as previously reported[30]. Cells were grown to 50–70% confluency and infected with recombinant adenovirus at a multiplicity of infection (MOI) of 15–30 for the indicated times. GFP- or LacZ-expressing adenovirus (Ad-GFP or Ad-LacZ) was used as control. cDNAs of ASC-PYD and ASC-CARD were cut out from the GFP fusion constructs with *Eco*RI and *Sal*I and ligated into pGEX4T-1 vectors (Amersham, Piscataway, NJ). GST-fused proteins were amplified using glutathione beads from *Escherichia coli* (BL21) under isopropyl β-D-thiogalactosidase (IPTG) stimulation.

Cell lines and culture conditions. MCF7, IMR90, IMR90-E1A, U2OS, Saos2, EJ and HCT116 cells were cultured in DMEM containing 10% foetal bovine serum (FBS) (Invitrogen, Carlsbad,CA), 100 U ml^{-1} penicillin and 100 μg ml^{-1} strepto-mycin at 37 °C. EJ-p53 cells were cultured in the presence or absence of tetracy-cline (2 μg ml^{-1}). For drug treatment, cells were exposed to mitomycin *c* (MMC; Sigma, St Louis, MO) at a concentration of 2.5 μg ml^{-1}, etoposide at 50 μM, TNFα (35 ng ml^{-1}) with cycloheximide (5 μg ml^{-1}) and camptothecin (CPT) at 300 nM for 12–48 h. Cells were treated with γ-irradiation at a dose of 5 Gy.

Chromatin immunoprecipitation (ChIP). Saos2 cells were seeded in p100 dishes at 40% density the day before adenovirus infection. At 24 h after Ad-p53 infection, cells were formaldehyde cross-linked and ChIP was performed according to the manufacturer's instructions using the Chromatin Immunoprecipitation Assay Kit (Upstate Biotechnology, Lake Placid, NY) with the following specifications/modifications: immunoprecipitation was per-formed at 4 °C overnight using 2 μg anti-p53 FL393 polyclonal antibody (Santa Cruz Biotechnology, Santa Cruz, CA) and HA-tag antibody (Y-11; Santa Cruz Biotechnology) as a negative control. PCR amplification was performed using primers (5′-TGCTCCAATAAACCCAGTGA-3′, 5′-AAGGCGCTTCCTTACTA-CACC-3′), designed to give a 225-bp product, including the p53-responsive ele-ment in the ASC promoter. The primers for the p21 promoter region, including the p53-responsive element, (5′-CTGAAAGCTGACTGCCCCTA-3′, 5′-TCTC-CTACCATCCCCTTCCTC-3′; 417-bp product) were also used as a positive control. The PCR protocol was 35 cycles of a 45-s denaturation step at 94 °C, a 1-min annealing step at 54 °C and a 1-min extension step at 72 °C.

Expression array screening. Affymetrix GeneChips were used for hybridization (Affymetrix, Santa Clara, CA). Two sets of human expression arrays (human genome U95A, Affymetrix) were hybridized with fluorescently labelled cRNA probes derived from total RNAs extracted from EJ-p53 cells grown in the pres-ence or absence of tetracycline for 1 and 2 days, respectively.

Flow cytometry and apoptosis assays. Cells were pelleted and washed with PBS. Ice-cold 80% ethanol was then added dropwise over the pellets with periodic vortexing to mix cells. After fixation, propidium iodide was added to 50 μg ml^{-1} in PBS and samples were analysed by flow cytometry. Sub-G1 populations were analysed using the CellQuest program. Trypan blue was added to cell pel-lets and stained cells were counted as dead.

Northern blot analysis. Total RNA was extracted, denatured, electrophoresed through a 1% agarose–formaldehyde gel and transferred to a nylon membrane

(BioRad, Hercules, CA). Hybridization was performed with ^{32}P-labeled probes prepared by the randomly primed DNA labelling method.

Western blot, immunoprecipitation and GST pull-down assay. Cells were lysed in lysis buffer (20 mM Tris-HCl at pH 7.4, 5 mM EDTA, 10 mM Na$_4$P$_2$O$_7$, 100 mM NaF, 2 mM Na$_3$VO$_4$, 1% NP-40, 1 mM phenyl methyl-sulphonyl fluoride (PMSF), 10 μg ml^{-1} aprotinin and 10 μg ml^{-1} leupeptin). Equal amount of total cellular proteins per sample was subjected to SDS–PAGE and transferred to a nitrocellulose membrane (Invitrogen). Immunoprecipitation was performed using 500 μg cell extracts incubated with anti-Myc monoclonal (9E10, agarose conjugate; Covance, Princeton, NJ), anti-Bax monoclonal (6A7; BD Pharmingen, San Jose, CA), anti-HA monoclonal (Y-11 agarose conjugate; Covance) and anti-Bax polyclonal (N-20; Santa Cruz) antibodies. For immunoprecipitation with Bax antibodies, 20 μl of protein A–agarose beads (Sigma) were added. The beads were washed and subjected to SDS–PAGE and immunoblotting. GST pull-down assay was performed using 500 μg cell extracts. Antibodies for immunoblotting included anti-p53 (Ab-6; Oncogene, Boston, MA), phospho-p53 (Ser15; Cell Signaling, Beverly, MA), p21 (Ab-1; Oncogene), ASC (MBL, Nagoya, Japan), β-actin (AC-15,;Sigma), Myc tag (9E10; Santa Cruz), Flag (M2; Sigma), HA (11; Covance), Bax (N-20; Santa Cruz), Bcl-X$_L$ (Cell Signaling), Noxa (Ab-1; Oncogene), Bak (2-14; Calbiochem), GFP (Clontech, Palo Alto, CA), GST (Amersham), caspase-2 (C-20; Santa Cruz or Chemicon), caspase-3, -7 and -9 (Cell Signaling), cytochrome *c* (2C12; BD Pharmingen) and NADH-ubiquinone oxidoreductase (Complex I, 20C11; Molecular Probes, Eugene, OR). Bands were detected using the ECL chemiluminescence detection method (Amersham). For Bax configuration analysis, cells were lysed in Chaps buffer[26]. The soluble fraction was immunoprecipitated with anti-Bax monoclonal antibody (6A7, BD Pharmingen) before western blot analysis with the N-20 anti-Bax antibody.

Immunostaining. Cells were fixed in 4% formaldehyde before permeabilization in 0.2% Triton X-100. Primary antibodies used were anti-Myc mouse monoclonal (9E10; Santa Cruz) and anti-HA rabbit polyclonal (Y-11; Santa Cruz), anti-ASC monoclonal (MBL) and anti-Bax polyclonal (N-20; Santa Cruz). Secondary antibodies were FITC-conjugated for mouse IgG (Jackson Immunoresearch) and Rhodamine Red- and FITC-conjugated for rabbit IgG (Molecular Probes). Mitochondria were stained by MitoTracker Orange (Molecular Probes). All images were collected by a confocal laser scanning microscope and processed using Adobe Photoshop software.

Mitochondrial preparation and cytosolic extracts. Cells were lysed in buffer (250 mM sucrose, 20 mM HEPES, 10 mM KCL, 1.5 mM MgCl$_2$, 1 mM EDTA, 1 mM EGTA, 1 mM dithiothreitol, 1 mM PMSF, 10 μg ml^{-1} aprotinin, and 10 μg ml^{-1} leupeptin at pH 7.5) and incubated for 30 min on ice. Cells were homogenized by 30 strokes in a 22-guage needle or Dounce-homogenized. Homogenates were centrifuged at 750*g* for 10 min at 4 °C. Supernatants were centrifuged at 10,000*g* for 15 min at 4 °C to collect the mitochondrial pellets.

siRNA experiments. Sense and anti-sense oligonucleotides corresponding to the following cDNA sequences were purchased from Dharmacon: AAGAT-GCGGAAGCTCTTCAGT (nucleotides 472–492) for ASC, GACTCCAGTG-GTAATCTAC (nucleotides 775–793) for p53, TGAGTACTTCACCAAGATT (nucleotides 324–342) for Bak and AAACAGCTGTTGTTGAGCGAA (nucleotides 94–114) for caspase-2. Cells were transfected with Oligofectamine (Invitrogen) or Nucleofector (AMAXA, program p-22) according to the manufacturer's protocol in the presence of siRNA. siRNA against luciferase (CTGACGCGGAATACTTCGA) was used as a control.

Note: Supplementary Information is available on the Nature Cell Biology website.

1. Pawlowski, K., Pio, F., Chu, Z., Reed, J. C. & Godzik, A. PAAD — a new protein domain associated with apoptosis, cancer and autoimmune diseases. *Trends Biochem. Sci.* **26**, 85–87 (2001).
2. Masumoto, J. *et al.* ASC, a novel 22-kDa protein, aggregates during apoptosis of human promyelocytic leukemia HL-60 cells. *J. Biol. Chem.* **274**, 33825–33838 (1999).
3. Conway, K. E. *et al.* TMS1, a novel proapoptotic caspase recruitment domain protein, is a target of methylation-induced gene silencing in human breast cancers. *Cancer Res.* **60**, 6236–6242 (2000).
4. Stehlik, C. *et al.* The PAAD/PYRIN-family protein ASC is a dual regulator of a conserved step in nuclear factor κB activation pathways. *J. Exp. Med.* **196**, 1605–1615 (2002).
5. Chae, J. J. *et al.* Targeted disruption of Pyrin, the FMF protein, causes heightened sensitivity to endotoxin and a defect in macrophage. *Mol. Cell* **11**, 591–604 (2003).
6. McConnell, B. B. & Vertino, P. M. Activation of a caspase-9-mediated apoptotic pathway by subcellular redistribution of the novel caspase recruitment domain protein TMS1. *Cancer Res.* **60**, 6243–6247 (2000).
7. Shiohara, M. *et al.* ASC, which is composed of a PYD and a CARD, is up-regulated by inflammation and apoptosis in human neutrophils. *Biochem. Biophys. Res. Commun.* **293**, 1314–1318 (2002).
8. Vogelstein, B., Lane, D. & Levine, A. J. Surfing the p53 network. *Nature* **408**, 307–310 (2000).
9. Oren, M. Decision making by p53: life, death and cancer. *Cell Death Differ.* **10**, 431–442 (2003).
10. Miyashita, T. & Reed, J. C. Tumor suppressor p53 is a direct transcriptional activator of the human bax gene. *Cell* **80**, 293–299 (1995).
11. Wei, M. C. *et al.* Proapoptotic BAX and BAK: a requisite gateway to mitochondrial dysfunction and death. *Science* **292**, 727–730 (2001).
12. Gross, A., McDonnell, J. M. & Korsmeyer, S. J. BCL-2 family members and the mitochondria in apoptosis. *Genes Dev.* **13**, 1899–1911 (1999).
13. Zhang, L., Yu, J., Park, B. H., Kinzler, K. W. & Vogelstein, B. Role of Bax in the apoptotic response to anticancer agents. *Science* **290**, 989–992 (2000).
14. Fearnhead, H. O. *et al.* Oncogene-dependent apoptosis is mediated by caspase-9. *Proc. Natl Acad. Sci. U S A* **95**, 13664–13669 (1998).
15. Lindsten, T. *et al.* The combined functions of proapoptotic Bcl-2 family members bak and bax are essential for normal development of multiple tissues. *Mol. Cell* **6**, 1389–1399 (2000).
16. Zong, W. X., Lindsten, T., Ross, A. J., MacGregor, G. R. & Thompson, C. B. BH3-only proteins that bind pro-survival Bcl-2 family members fail to induce apoptosis in the absence of Bax and Bak. *Genes Dev.* **15**, 1481–1486 (2001).
17. Li, H. & Yuan, J. Deciphering the pathways of life and death. *Curr. Opin. Cell Biol.* **11**, 261–266 (1999).
18. Coultas, L. & Strasser, A. The role of the Bcl-2 protein family in cancer. *Semin. Cancer Biol.* **13**, 115–123 (2003).
19. Green, D. R. & Reed, J. C. Mitochondria and apoptosis. *Science* **281**, 1309–1312 (1998).
20. Hsu, Y. T. & Youle, R. J. Bax in murine thymus is a soluble monomeric protein that displays differential detergent-induced conformations. *J. Biol. Chem.* **273**, 10777–10783 (1998).
21. Nechushtan, A., Smith, C. L., Hsu, Y. T. & Youle, R. J. Conformation of the Bax C-terminus regulates subcellular location and cell death. *EMBO J.* **18**, 2330–2341 (1999).
22. Suzuki, M., Youle, R. J. & Tjandra, N. Structure of Bax: coregulation of dimer formation and intracellular localization. *Cell* **103**, 645–654 (2000).
23. Marsden, V. S. *et al.* Apoptosis initiated by Bcl-2-regulated caspase activation independently of the cytochrome c/Apaf-1/caspase-9 apoptosome. *Nature* **419**, 634–637 (2002).
24. Masumoto, J. *et al.* ASC is an activating adaptor for NF-κB and caspase-8-dependent apoptosis. *Biochem. Biophys. Res. Commun.* **303**, 69–73 (2003).
25. Lassus, P., Opitz-Araya, X. & Lazebnik, Y. Requirement for caspase-2 in stress-induced apoptosis before mitochondrial permeabilization. *Science* **297**, 1352–1354 (2002).
26. Sawada, M. *et al.* Ku70 suppresses the apoptotic translocation of Bax to mitochondria. *Nature Cell Biol.* **5**, 320–329 (2003).
27. Guo, B. *et al.* Humanin peptide suppresses apoptosis by interfering with Bax activation. *Nature* **423**, 456–461 (2003).
28. Stimson, K. M. & Vertino, P. M. Methylation-mediated silencing of TMS1/ASC is accompanied by histone hypoacetylation and CpG island-localized changes in chromatin architecture. *J. Biol. Chem.* **277**, 4951–4958 (2002).
29. Masumoto, J., Taniguchi, S. & Sagara, J. Pyrin N-terminal homology domain- and caspase recruitment domain-dependent oligomerization of ASC. *Biochem. Biophys. Res. Commun.* **280**, 652–655 (2001).
30. He, T. *et al.* A simplified system for generating recombinant adenoviruses. *Proc. Natl. Acad. Sci. USA* **95**, 2509–2514 (1998).
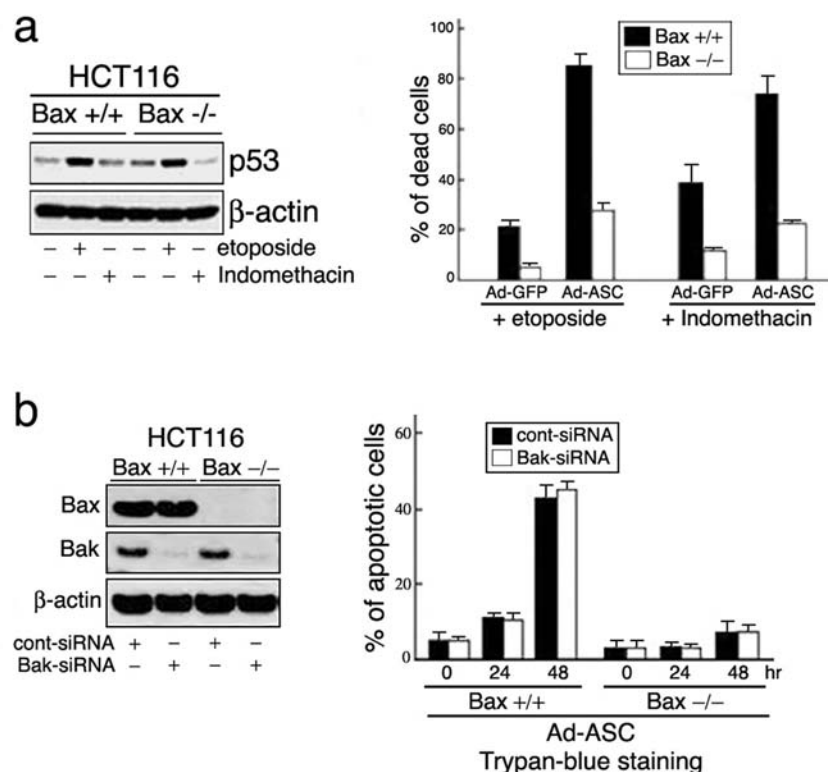
nature
cell biology

Figure S1. Effect of ASC overexpression on apoptosis induced by apoptotic drugs (a). Bax+/+ or Bax–/– HCT116 cells were infected with Ad-ASC or Ad-GFP, treated with etoposide (50μM) (p53-dependent) and indomethacin (500μM) (p53-independent), respectively, and incubated for 24 hours. p53 expression in cells treated with etoposide or indomethacin was assessed by Western blots. The percentage of dead cells was then measured by Trypan-blue exclusion analysis. The apoptotic population (sub-G1 population) was also measured by FACS analysis. Error bars indicate $\pm$ SD of three independent experiments with duplicate plates. b. ASC-induced apoptosis does not require Bak. Bax+/+ or Bax–/– HCT116 cells were transfected with siRNA oligos targeting Bak or control siRNA oligos (luciferase). After 36 hours, cells were infected with either Ad-ASC or Ad-GFP for 36 hours then the apoptotic population was measured by FACS analysis. Trypan-blue exclusion was also performed at the indicated times. The left panel shows Western blot analysis prepared from cells transfected with either Bak- or luciferase-siRNA.
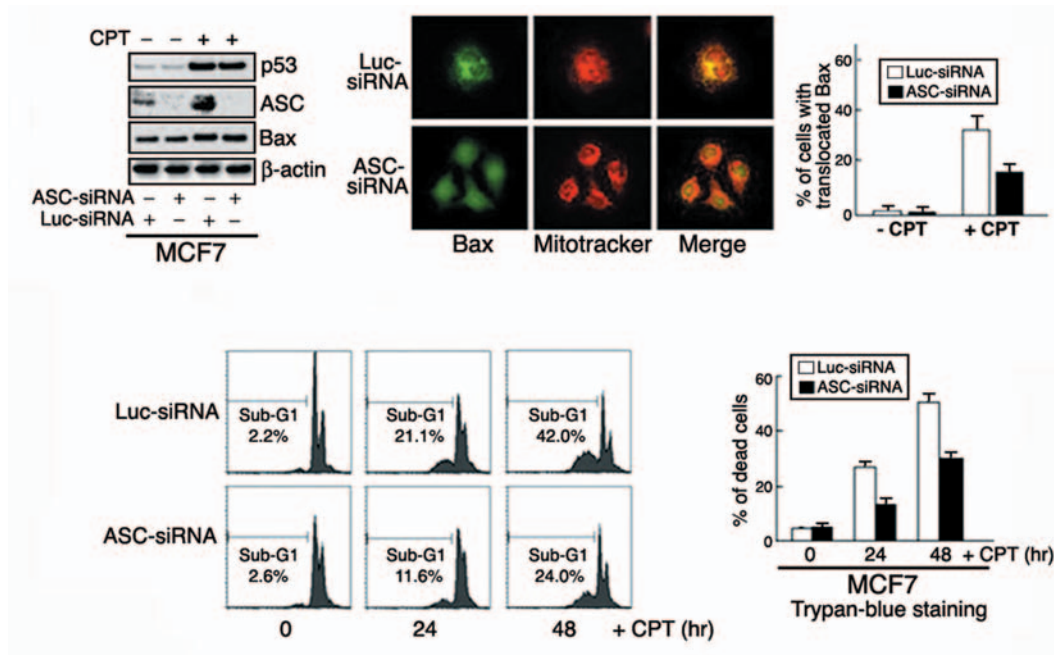
SUPPLEMENTARY INFORMATION

Figure S2. Effects of ASC on p53- or DNA damage-induced Bax translocation and apoptosis in MCF7 cells. MCF7 cells were transfected with siRNA to ASC or luciferase(control). Forty eight hours after transfection cells were treated with camptothecin (CPT, 300nM) or DMSO (a solvent of the choice). After 24 hours of treatment, cells were collected for immunoblot analysis (a) using antibodies to p53, ASC, Bax and β-actin. A portion of the cells was immunostained with antibodies to Bax (green) (b, the left panel). Mitochondria were stained with MitoTracker (red); the two images were overlaid (orange-yellow). Bax translocation was determined by counting 100 to 150 cells for each cell population and is presented in the right panel (b, the right panel). Error bars indicate ± SD of three independent experiments. Effect of ASC inhibition on genotoxic stress-induced apoptosis was examined in MCF7 cells (c). The cells were transfected with siRNA and treated with 300nM CPT or DMSO as described in the main text, and the rate of apoptosis was determined by FACS analysis as well as Trypan-blue exclusion at the indicated times (c, the right panel).
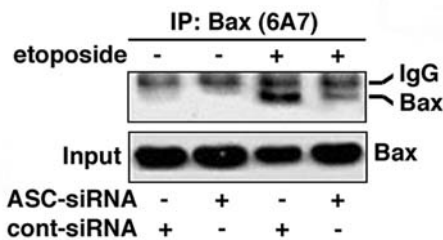

Figure S3. ASC-induced conformation change of the Bax protein. After 12 hours with or without etoposide treatment, the IMR90-E1A cells were also lysed in the presence of Chaps and immunoprecipitation with anti-Bax monoclonal antibody (clone 6A7) was performed and followed by Western blotting using anti-Bax polyclonal antibody (N-20). Note that the inhibition of ASC decreased the apoptosis-induced conformational change of Bax.
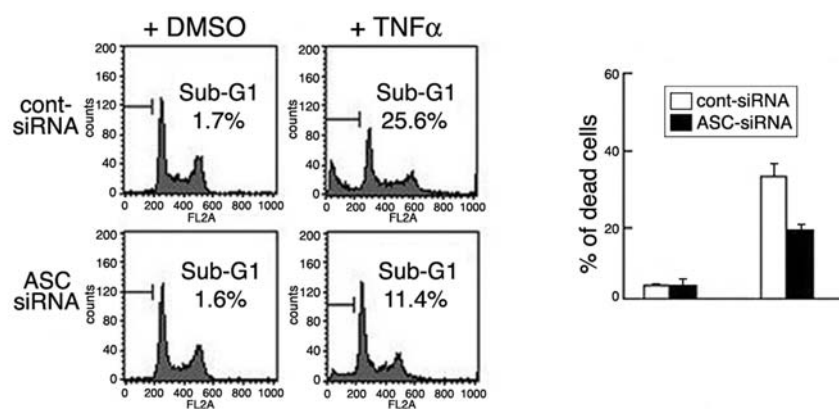
Figure S4. ASC repression compromises TNFα-mediated apoptosis. IMR90-E1A cells were transfected with siRNA oligos targeting ASC or control siRNA oligos (luciferase) for 2 days, then treated with TNFα (35ng/ml) in conjunction with 5μg/ml of cycloheximide for 12 hours. The apoptotic population (sub-G1 population, left panel) was also measured by FACS analysis using the same cells. The percentage of dead cells was measured by Trypan-blue exclusion analysis (right panel). Error bars indicate ± SD of three independent experiments with duplicate plates.